Published in final edited form as:
Curr Biol. 2008 January 8; 18(1): 63–68.

The Peroxin Loss-of-Function Mutation *abstinence by mutual consent* Disrupts Male-Female Gametophyte Recognition[1]

Aurélien Boisson-Dernier*, **Sabine Frietsch**[2,3], **Tae-Houn Kim**[3], **Marie B. Dizon**, and **Julian I. Schroeder***

Division of Biological Sciences, Cell and Developmental Biology Section, and Center for Molecular Genetics, University of California, San Diego, 9500 Gilman Drive, La Jolla, California 92093-0116, USA

Summary

In eukaryotes, fertilization relies on complex and specialized mechanisms that achieve the precise delivery of the male gamete to the female gamete and their subsequent union [1–4]. In flowering plants, the haploid male gametophyte or pollen tube (PT) [5] carries two non-motile sperm cells to the female gametophyte (FG) or embryo sac [6] during a long assisted journey through the maternal tissues [7–10]. In *Arabidopsis*, typically one PT reaches one of the two synergids of the FG (Figure 1A) where it terminates its growth and delivers the sperm cells, a poorly understood process called pollen tube reception. Here, we report the isolation and characterization of the *Arabidopsis* mutant *abstinence by mutual consent.* Interestingly, pollen tube reception is impaired only when an *amc* pollen tube reaches an *amc* female gametophyte resulting in pollen tube overgrowth and completely preventing sperm discharge and the development of homozygous mutants. Moreover, we show that *AMC* is strongly and transiently expressed in both male and female gametophytes during fertilization and that AMC functions in gametophytes as a peroxin essential for protein import into peroxisomes. These findings show that peroxisomes play an unexpected key role in gametophyte recognition and implicate a diffusible signal emanating from either gametophytes that is required for pollen tube discharge.

Results and Discussion

To date, the molecular and genetic mechanisms of pollen tube reception are poorly understood and only the *Arabidopsis feronia/sirene* mutations have been reported to specifically disrupt this complex process [11,12]. In the *feronia*/*sirene* female gametophytic mutants, PTs reach the micropyle but are unable to stop their growth and are unable to burst demonstrating that the FG participates in the control of PT reception [11,12]. With the recent characterization of FER/SIR as a synergid-expressed, plasma membrane-localized receptor-like kinase [13], one possible model for pollen tube reception emerges: when the PT reaches the synergids, a ligand from the PT triggers upon binding to the FER extracellular domain a signaling cascade enabling

[1]This research was supported by National Institute of Health (R01GM060396) and by National Science Foundation (MCB0417118) grants to J.I.S.

* Corresponding authors; emails : julian@biomail.ucsd.edu; aboisson@biomail.ucsd.edu; fax 858-534-7108.
[2]Present address: University of Nevada, Reno, Biochemistry Department MS200, 1664 N. Virginia St., Reno, Nevada 89557, USA
[3]These authors contributed equally to this work

the female gametophyte to prepare itself for fertilization [13,14]. In return, the FG would signal back to the pollen tube to stop growing and discharge its sperm cells [13,14]. Here, we have identified and characterized a T-DNA insertional *Arabidopsis* mutant that exhibits defective pollen tube reception only when a mutant pollen tube interacts with a mutant embryo sac resulting in pollen tube overgrowth and the absence of homozygous individuals. Therefore, we named this self-sterile mutant *amc*/+ for *abstinence by mutual consent*.

amc mutant does not produce homozygous individuals

After screening more than 500 progenies from heterozygous *amc*/+ T2 plants, we were unable to identify plants homozygous for the T-DNA insertion in the *AMC* gene (Table 1). Unlike immature siliques of wild-type plants filled to 94% with green seeds, self-pollinated heterozygous *amc*/+ siliques were only filled to 76% with green seeds and contained also 24% of white shriveled ovules randomly located within the siliques (Table 1; Figure 1B). Within *amc*/+ progeny, the segregation of the *amc* allele (Table 1) or the Kanamycin marker from the T-DNA (Table S1) resulted in ~2:1 ratio instead of the expected 3:1. The absence of homozygous plants, the seed-set silique phenotype as well as the distorted segregation ratio were still occurring after four successive backcrosses and all the Kanamycin-resistant plants (n>300) exhibited the incomplete seed-set phenotype.

Reciprocal crosses to the wild-type were performed to determine the transmission efficiency (TE) of the *amc* allele. While the transmission by the female gametophyte was not significantly affected (83%; Table 1; χ^2= 0.49, 0.5>P>0.4), the TE by the male gametophyte was moderately but significantly reduced (51%; Table 1; P<0.01, χ^2). Furthermore, siliques resulting from either reciprocal crosses had a wild-type-like full-seed set (Table 1) indicating that the reduced male TE could not alone account for the incomplete silique seed-set observed during *amc*/+ self-pollination. Since the *amc* mutation is fully penetrant and neither affects pollen germination nor PT growth *in vitro* (see below and Supplementary Data, Figure S7), one possible explanation for the reduced male TE is that *amc* mutant pollen tubes are less efficient than wild-type PTs in targeting ovules. More importantly, these findings indicate that the observed ovule abortion within *amc*/+ siliques is caused by an embryonic defect or a synergistic defect from both male and female gametophytes. Considering the reduced male TE, within the progeny of self-pollinated *amc*/+ plants, homozygous *amc/amc* individuals should be observed at a frequency of 15.3% (Table S2; 0.337 × 0.453 = 0.153) instead of the expected 25% (0.5 × 0.5 = 0.25). However, such homozygous plants were never identified (n=524, Table 1).

AMC encodes an atypical peroxin

The *amc*/+ mutant carries a T-DNA insertion in exon III of the At3g07560 gene that triggered a 16-bp deletion suggesting that *amc* is a frame-shifted disruption allele (Figure 1C). Introduction of a wild-type copy of At3g07560 rescued the seed-set phenotype in 13 out of 16 *amc*/+ T1 lines. The absence of homozygotes and the distorted segregation ratio observed for *amc*/+ plants and their progeny were also complemented (see Supplemental Data) demonstrating that At3g07560 corresponds to the *AMC* gene. *AMC* encodes a protein of 304 amino acids and is a single gene in *Arabidopsis thaliana*. Recently, Mano and colleagues reported that the *aberrant peroxisome morphology 2 (apm2)* mutant which carries a point mutation in the C-terminal region of AMC (Figure 1C), from here on named APM2/AMC, exhibits weak peroxin-deficient phenotypes [15]. They also showed that APM2/AMC is targeted to peroxisomes and exhibits limited similarity to the SH3 domain-containing peroxin PEX13 from various organisms (see Supplemental Data, Figure S1B) [15]. Most peroxisomal proteins use either Peroxisome Targeted Signal 1 (PTS1) or PTS2 to enter peroxisomes [16, 17] and PEX13 has been shown to function in both PTS1- and PTS2-dependent import pathways [18,19]. However, our detailed APM2/AMC sequence analyses indicated that

APM2/AMC does not have an SH3 domain and may not be a direct ortholog of PEX13 (see Supplemental Data, Figure S1).

APM2/AMC is essential for pollen tube discharge

To investigate the cause of the incomplete seed set of selfed *amc*/+ siliques, we analyzed developing seeds in *amc*/+ siliques using Nomarski optics but could not observe any obvious fertilization signs in the senescing ovules (see Supplemental Data, Figure S2A). Moreover, within *amc*/+ siliques the small senescing ovules were targeted by PTs as frequently as the normal young seeds (see Supplemental Data, Figure S2B) suggesting that the incomplete seed set observed for the *amc*/+ siliques is the result of ovules normally targeted by PTs that remain unfertilized. Therefore it is very likely that the *amc* mutation triggers defects in fertilization.

To visualize the effect of the *amc* mutation on the interactions between gametophytes, transgenic wild-type and *amc*/+ plants expressing the YFP (Yellow Fluorescent Protein) reporter driven by the pollen specific *ACA9* promoter were generated [20]. When wild-type YFP-expressing pollen was deposited on wild-type pistils, two distinct interactions were observed 19–24h after manual pollination. In approximately 64% of the wild-type events, one PT tip reached the vicinity of the micropylar side of the synergids (n=216 out of 336; Figure 2A). This could be interpreted as the PT having reached the synergids and not having discharged yet or the transient discharge having already occurred. In the remaining interactions, as previously described [21], a classical transient discharge of one fluorescent pollen tube content within the receptive synergid could be observed (n=120 out of 336; Figure 2B–D). In manual crosses between pollen and pistils from *amc*/+ plants, we also witnessed PTs at the micropylar side of synergids (n=275 out of 468) as well as classical discharges (n=130 out of 468). Surprisingly, in the remaining 13.5% of the interactions (n=63 out of 468), the pollen tube normally reached the synergids but then, instead of terminating its growth and bursting, the PT invaded the micropylar part of the ovule by growing continuously and forming coils and/or branching (Figure 2E–H). Moreover, during these mutant interactions, synergid cell degeneration appeared to be delayed although PTs and synergids were in close contact (see Supplemental Data, Figure S3) [22]. Such severe PT overgrowth was never observed during reciprocal crosses of *amc*/+ with wild-type (n>300 for both cross directions), which is consistent with the wild-type-like full seed set of the siliques resulting from these crosses (Table 1).

Among the interactions between *amc*/+ pollen and *amc*/+ pistils, the invading pollen tube phenotype was observed in 13.5% of the analyzed events which was not significantly different from the 15.3% (χ^2= 1.22, 0.3>P>0.2) expected for the interaction between an *amc* mutant pollen and an *amc* mutant ovule (see above and Table S2). Thus, our data provide strong evidence that during the interaction between an *amc* mutant pollen tube and an *amc* mutant embryo sac, the PT keeps growing and does not deliver its sperm cells, therefore preventing fertilization and the development of an *amc/amc* homozygous individual.

While wild-type ovules typically receive only one pollen tube [9], an *amc* ovule receiving an *amc* PT appears to continue to attract other pollen tubes since we frequently observed more than one PT within the FGs with the invading pollen mutant phenotype (n=28 out of 63; Figure 2E, arrows).

Interestingly, the *fer/sir* mutants exhibit very similar pollen tube invading phenotypes as the ones observed for *amc*/+, although in the case of the *feronia/sirene* mutants, they are only attributable to the mutant FGs [11,12]. Therefore, our data provide genetic evidence that pollen tubes are not just a passive sperm carrier controlled by the FG during pollen tube reception. Strikingly the failure of pollen tube reception in *feronia/sirene* FGs or between *amc* PTs and *amc* FGs appeared to have the same immediate consequences: the receptive synergid does not

degenerate on arrival of the pollen tube and the female gametophyte continues to attract other PTs (Figure 2E and S3C) [11,12].

Since *feronia* female gametophytes are unable to correctly receive wild-type PTs, one could argue that the PT overgrowth phenotype is a consequence of mutant FGs structurally or physiologically unfit to receive pollen tubes [11,12]. However, the new finding that *amc* FGs are fully competent to receive wild-type PTs (Table 1) added to the observations that *feronia* and *amc* female gametophytes correctly expressed synergid-specific markers and did not reveal any structural defect (see Supplemental Data, Figure S3) [11] rule out this possibility. An emerging alternative model for the pollen tube overgrowth observed in these mutants is that a FER receptor kinase-dependent recognition/communication system between male and female gametophytes necessary for proper pollen tube reception is disrupted [13,14]. Analysis of the seed set of self-pollinated *fer*/+ *amc*/+ double mutant siliques suggests that the FER and APM2/AMC pathways are at least partially independent (see Supplemental Data and Table S3). The *amc* mutation may disrupt either the FER-dependent signaling pathway in the FG or the subsequent feed-back signaling pathway in the PT that leads to sperm discharge. Alternatively, redundant signals/molecules independent from the FER-dependent pathway and originating from either gametophytes could be required to create a unique niche suitable for sperm discharge.

APM2/AMC is expressed in both male and female gametophytes during fertilization

Consistent with publicly available ATH1 microarray data from various organs [23] and pollen transciptome studies [24,25] (Figure S4A), *APM2/AMC* expression was detected by semi-quantitative and quantitative real-time RT-PCR analyses in every organ tested but was particularly more abundant in pollen (Figure 3A). In transgenic lines expressing the beta-glucuronidase gene (*GUS*) driven by a 1.4 Kb –long *APM2/AMC* promoter, moderate GUS activity was present in a wide range of vegetative tissues (see Supplemental Data, Figure S4) and again, the strongest GUS signal was observed in the mature pollen grain (Figure 3B). Interestingly, in the unfertilized mature female gametophytes, GUS activity was induced by pollen deposition on the pistils (Figure 3C, see also Supplemental Data and Figure S4F for whole stained-pistil series during pollination). During fertilization, both female (asterisk) and male (arrow) gametophytes were intensely stained in clear contrast to the surrounding diploid tissues (Figure 3D). However, after fertilization *APM2/AMC* promoter activity decreased dramatically as the young embryo developed (Figure 3E–F). Together, our data indicate that *APM2/AMC* is strongly expressed in both male and female gametophytes during fertilization, consistent with an important fertilization function for APM2/AMC in both gametophytes.

The *amc* mutation completely disrupts PTS1-dependent protein import into pollen peroxisomes

First, we confirmed the peroxisomal subcellular localization of APM2/AMC [15] in onion epidermal cells (see Supplemental Data, Figure S5). Moreover *APM2/AMC* antisense lines exhibited phenotypes in vegetative tissues that are characteristic of peroxin mutants deficient in photorespiration, a peroxisomal process requiring PTS1-dependent import (see Supplemental Data, Figure S6) [26–29]. Consistently, the protein import into peroxisomes via the PTS1-dependent pathway was indeed partially defective in the *APM2/AMC* antisense lines (see Supplemental Data, Figure S6), as reported for the weak *apm2* mutant [15]. Finally, we directly analyzed the effect of the *amc* null mutation on PTS1-dependent protein import into peroxisomes by transforming WT and *amc*/+ plants (in a *quartet* mutant background) [30] with the pollen peroxisome targeting pLAT52-CFP-PTS1 construct [31]. In WT plants heterozygous for the pLAT52-CFP-PTS1 fusion, all the fluorescent pollen grains exhibited fluorescence with a peroxisome-like punctuated pattern (Figure 4A, arrows; n>200). In clear contrast, pollen grains from *amc*/+ tetrads exhibited fluorescence exclusively either in

peroxisomes (Figure 4B, arrow; n=117 out of 242) or in the cytosol (Figure 4B, arrowhead; n=125 out of 242) in a 1:1 ratio expected for the segregation of the *amc* mutation (χ^2= 0.26, 0.7>P>0.5; see also Figure S7). Therefore, our results provide strong evidence that APM2/AMC functions as a peroxin in reproductive tissues and more importantly that APM2/AMC is essential for the PTS1-dependent import pathway. Although the precise relation of APM2/AMC to other peroxins requires further investigation, analysis of the strong *amc* allele definitely establishes APM2/AMC as a core component of the plant peroxisomal matrix protein import machinery.

The present detailed analysis of the complete loss-of-function *amc* allele also reveals for the first time that functional peroxisomes must be present in either the male or the female gametophyte for pollen tube reception to take place. It is therefore conceivable that the mislocalization of a protein normally targeted to the peroxisomes can affect pollen tube reception. Peroxisomes in plants are known to maintain a cellular redox balance and are a source of a large range of signaling molecules such as jasmonic acid, salicylic acid, indole acetic acid, reactive oxygen species (ROS) and nitric oxide (NO) [32,33]. In animals, ROS and NO are known to play key roles in fertilization-related processes such as capacitation, the acrosome reaction, oocyte activation, ovulation and fertilization itself [34–37]. In plants little is known about these signaling molecules during fertilization. Recently peroxisomes have been shown to be the source of NO production in pollen tubes and NO was able to reorient pollen tube growth *in vitro* [31]. One possible model for our findings is that a signal/molecule originating from gametophyte peroxisomes, for example a diffusible gas or small molecules such as NO or ROS, is required for the dialogue between gametophytes that lead to sperm discharge. In this context, the impairment in production/release of the molecule in one gametophyte could be rescued by diffusion of the molecule from the other nearby gametophyte. Future isolation of other mutants with defective pollen tube reception as well as the use of non invasive techniques to visualize ROS and NO production *in vivo* during fertilization should further the understanding of the peroxisome-dependent mechanisms that are critical for successful gametophyte-gametophyte communication and sperm discharge.

Experimental Procedures

Mutant Line Genotyping

For standard methods see Supplemental Experimental Procedures. The *amc* allele of the At3g07560 gene was obtained from the Signal Collection at the Salk Institute (La Jolla, CA, USA) [38] and corresponds to the Salk_055083 line. Genotyping PCR reactions for mutants were performed using a combination of primers b and c (5′-ggcagtcctcctaaaccttggg-3′ and 5′-ccatcgcaccaccaccatacatgcc-3′), b and LBa1 (5′-tggttcacgtagtgggccatcg-3) and finally c and RBa1 (5′-gctcattaaactccagaaacccgcg-3′) and amplified products were sequenced (Figure 1C).

Constructs and generation of transgenic plants

The binary vectors constructed and described below were introduced into *Agrobacterium tumefaciens* strain GV3101 by electroporation, which was then used to transform by floral dipping [39] wild-type or Kanamycin resistant *amc*/+ plants in a *quartet* mutant background [30,40,41].

pACA9-DsRED as well as pACA9-D3 (the cameleon reporter containing the YFP) [42] and pMYB98-D3 constructs were generated and kindly provided by Jeffrey Harper (Biochemistry Department, University of Nevada, Reno, Nevada, USA).

For the *APM2/AMC* gene promoter *GUS* reporter fusion, a 1392 bp fragment of the *APM2/AMC* locus was PCR-amplified from the F21O3 BAC using 5′-

actaatcaataaagcttatacacgaagaagg-3′ and 5′-gctaacctgcaggatccgacgccatatatc-3′ primers introducing the *Hind*III and *BamH*I sites (underlined) respectively and cloned into pGEM®-T Easy vector (Promega, Madison, USA) and sequenced. The 1392 bp fragment was then sub-cloned into the binary plant vector pLP100 [43] to generate a precise transcriptional fusion with the *gusA* reporter gene using *Hind*III and *BamH*I sites.

The pLAT52-CFP-PTS1 fusion in a pBluescript SKII vector [31] was kindly provided by Ana Silva and José Feijó (Fundação Calouste Gulbenkian, Instituto Gulbenkian de Ciência, Lisboa, Portugal). pLAT52-CFP-PTS1 was extracted by a *Kpn*I/*Sac*I digestion and then cloned into the *Kpn*I/*Sac*I cut binary pGreenII-0179 vector [44] conferring resistance to Hygromycin.

Microscopic phenotyping of wild-type and *amc*/+ mutant pollen/ovule interactions

For YFP- or DsRED-expressing pollen and YFP-expressing synergid cell observations, 19 to 24h after manual pollination, pistils were glued to a slide and cut along the replum with a micro-knife (Fine Science Tools, Foster City, California) under a dissecting microscope. The valves were carefully removed so that only the stigma, and the septum with the attached ovules remained on the slide which were submerged in 20% glycerol. Fluorescence imaging was acquired by spinning-disc confocal microscopy using a QLC100 confocal scanning unit (Solamere Technology Group, Salt Lake City, UT, USA) linked to a NIKON Eclipse TE 2000-U bright field microscope (Tokyo, Japan) and an argon laser (500 M Select, Laserphysics, West Jordan, UT, USA). Images were captured with an electron multiplying charge-coupled device (EMCCD) camera (Cascade II:512, Photometrics, Tucson, AZ, USA) using Metamorph software (Universal Imaging, Downington, PA, USA). For YFP observation, laser excitation was 488 nm and YFP fluorescence was selected in the green channel with a band-pass 500–550 nm filter. For DsRED or auto-fluorescence, laser excitation was 568 nm and fluorescence was selected in the red channel (converted to magenta) with a band-pass 580–650 nm filter. Z-stacks with 0.5 to 1 μm intervals were recorded for each channel, processed with the Metamorph stack arithmetic “best focus” function and then overlaid.

CFP-PTS1 fluorescence imaging

Pollen tetrads of wild-type and *amc*/+ T1 Hygromycin resistant plants expressing the pLAT52-CFP-PTS1 fusion were deposited on slides and submerged in 20% glycerol. Fluorescent pollen grains from the tetrads were then counted and examined by CLSM with the same set-up as for the observations of the YFP-expressing pollen except laser excitation was 440 nm and fluorescence was selected with a band-pass 440–514 nm filter. *In vitro* pollen germination and pollen tube growth assays (Supplemental Data and Figure S7) were carried out as previously described [45,46].

Supplementary Material

Refer to Web version on PubMed Central for supplementary material.

Acknowledgements

We thank Jeffrey Harper (University of Nevada, Reno, Nevada, USA) and Yunde Zhao (UCSD) for comments on the manuscript, Jean Colcombet (UCSD) for general discussion, Mingda Yan and Suresh Subramani (UCSD) for PEX13-related discussions, Jeff Long (The Salk Institute, La Jolla, California, USA) for DIC microscopy recommendations, Niko Geldner (The Salk Institute) for initiation to the Leica SP2 confocal microscope. We are very grateful to Jeffrey Harper (UNR) for generating and providing us with the pACA9-D3, pACA9-DsRED and pMYB98-D3 constructs. This work was supported by National Institutes of Health Grant R01 GM060396 and National Science Foundation grant MCB 0417118 to J.I.S. S.F. was supported by a “Boehringer Ingelheim Fonds” fellowship and NIH grant # R01 GM070813 to Jeffrey Harper.

References

1. Franklin-Tong VE. Signaling in pollination. Curr Opin Plant Biol 1999;2:490–495. [PubMed: 10607651]
2. Lord EM, Russell SD. The mechanisms of pollination and fertilization in plants. Annu Rev Cell Dev Biol 2002;18:81–105. [PubMed: 12142268]
3. Boavida LC, Vieira AM, Becker JD, Feijo JA. Gametophyte interaction and sexual reproduction: how plants make a zygote. Int J Dev Biol 2005;49:615–632. [PubMed: 16096969]
4. Dresselhaus T. Cell-cell communication during double fertilization. Curr Opin Plant Biol 2006;9:41–47. [PubMed: 16324880]
5. McCormick S. Control of male gametophyte development. Plant Cell 2004;16(Suppl):S142–S153. [PubMed: 15037731]
6. Yadegari R, Drews GN. Female gametophyte development. Plant Cell 2004;16(Suppl):S133–S141. [PubMed: 15075395]
7. McCormick S. Self-incompatibility and other pollen-pistil interactions. Curr Opin Plant Biol 1998;1:18–25. [PubMed: 10066554]
8. Higashiyama T, Kuroiwa H, Kuroiwa T. Pollen-tube guidance: beacons from the female gametophyte. Curr Opin Plant Biol 2003;6:36–41. [PubMed: 12495749]
9. Weterings K, Russell SD. Experimental analysis of the fertilization process. Plant Cell 2004;16 (Suppl):S107–S118. [PubMed: 15010512]
10. Johnson, MA.; Lord, ME. Extracellular guidance cues and intracellular signaling pathways that direct pollen tube growth. In: Malho, R., editor. The Pollen Tube: A Cellular and Molecular Perspective. Heidelberg: Springer; 2006. p. 223-242.
11. Huck N, Moore JM, Federer M, Grossniklaus U. The *Arabidopsis* mutant *feronia* disrupts the female gametophytic control of pollen tube reception. Development 2003;130:2149–2159. [PubMed: 12668629]
12. Rotman N, Rozier F, Boavida L, Dumas C, Berger F, Faure JE. Female control of male gamete delivery during fertilization in *Arabidopsis thaliana*. Curr Biol 2003;13:432–436. [PubMed: 12620194]
13. Escobar-Restrepo JM, Huck N, Kessler S, Gagliardini V, Gheyselinck J, Yang WC, Grossniklaus U. The FERONIA receptor-like kinase mediates male-female interactions during pollen tube reception. Science 2007;317:656–660. [PubMed: 17673660]
14. McCormick S. Plant science. Reproductive dialog Science 2007;317:606–607.
15. Mano S, Nakamori C, Nito K, Kondo M, Nishimura M. The *Arabidopsis pex12* and *pex13* mutants are defective in both PTS1- and PTS2-dependent protein transport to peroxisomes. Plant J 2006;47:604–618. [PubMed: 16813573]
16. Subramani S, Koller A, Snyder WB. Import of peroxisomal matrix and membrane proteins. Annu Rev Biochem 2000;69:399–418. [PubMed: 10966464]
17. Baker A, Sparkes IA. Peroxisome protein import: some answers, more questions. Curr Opin Plant Biol 2005;8:640–647. [PubMed: 16182600]
18. Schell-Steven A, Stein K, Amoros M, Landgraf C, Volkmer-Engert R, Rottensteiner H, Erdmann R. Identification of a novel, intraperoxisomal pex14-binding site in pex13: association of pex13 with the docking complex is essential for peroxisomal matrix protein import. Mol Cell Biol 2005;25:3007–3018. [PubMed: 15798189]
19. Williams C, Distel B. Pex13p: Docking or cargo handling protein? Biochim Biophys Acta 2006;1763:1585–1591. [PubMed: 17056133]
20. Schiott M, Romanowsky SM, Baekgaard L, Jakobsen MK, Palmgren MG, Harper JF. A plant plasma membrane Ca2+ pump is required for normal pollen tube growth and fertilization. Proc Natl Acad Sci USA 2004;101:9502–9507. [PubMed: 15197266]
21. Faure JE, Rotman N, Fortune P, Dumas C. Fertilization in *Arabidopsis thaliana* wild type: developmental stages and time course. Plant J 2002;30:481–488. [PubMed: 12028577]
22. Sandaklie-Nikolova L, Palanivelu R, King EJ, Copenhaver GP, Drews GN. Synergid cell death in *Arabidopsis* is triggered following direct interaction with the pollen tube. Plant Physiol 2007;144:1753–1762. [PubMed: 17545508]

23. Zimmermann P, Hirsch-Hoffmann M, Hennig L, Gruissem W. GENEVESTIGATOR. *Arabidopsis* microarray database and analysis toolbox. Plant Physiol 2004;136:2621–2632. [PubMed: 15375207]
24. Honys D, Twell D. Transcriptome analysis of haploid male gametophyte development in *Arabidopsis*. Genome Biol 2004;5:R85. [PubMed: 15535861]
25. Pina C, Pinto F, Feijo JA, Becker JD. Gene family analysis of the *Arabidopsis* pollen transcriptome reveals biological implications for cell growth, division control, and gene expression regulation. Plant Physiol 2005;138:744–756. [PubMed: 15908605]
26. Hayashi M, Nito K, Toriyama-Kato K, Kondo M, Yamaya T, Nishimura M. AtPex14p maintains peroxisomal functions by determining protein targeting to three kinds of plant peroxisomes. EMBO J 2000;19:5701–5710. [PubMed: 11060021]
27. Zolman BK, Bartel B. An *Arabidopsis* indole-3-butyric acid-response mutant defective in PEROXIN6, an apparent ATPase implicated in peroxisomal function. Proc Natl Acad Sci USA 2004;101:1786–1791. [PubMed: 14745029]
28. Fan J, Quan S, Orth T, Awai C, Chory J, Hu J. The *Arabidopsis PEX12* gene is required for peroxisome biogenesis and is essential for development. Plant Physiol 2005;139:231–239. [PubMed: 16113209]
29. Hayashi M, Yagi M, Nito K, Kamada T, Nishimura M. Differential contribution of two peroxisomal protein receptors to the maintenance of peroxisomal functions in *Arabidopsis*. J Biol Chem 2005;280:14829–14835. [PubMed: 15637057]
30. Preuss D, Rhee SY, Davis RW. Tetrad analysis possible in *Arabidopsis* with mutation of the *QUARTET* (*QRT*) genes. Science 1994;264:1458–1460. [PubMed: 8197459]
31. Prado AM, Porterfield DM, Feijo JA. Nitric oxide is involved in growth regulation and re-orientation of pollen tubes. Development 2004;131:2707–2714. [PubMed: 15128654]
32. Woodward AW, Bartel B. Auxin: regulation, action, and interaction. Ann Bot (Lond) 2005;95:707–735. [PubMed: 15749753]
33. Nyathi Y, Baker A. Plant peroxisomes as a source of signalling molecules. Biochim Biophys Acta 2006;1763:1478–1495. [PubMed: 17030442]
34. Herrero MB, de Lamirande E, Gagnon C. Nitric oxide is a signaling molecule in spermatozoa. Curr Pharm Des 2003;9:419–425. [PubMed: 12570819]
35. Baker MA, Aitken RJ. The importance of redox regulated pathways in sperm cell biology. Mol Cell Endocrinol 2004;216:47–54. [PubMed: 15109744]
36. Kuo RC, Baxter GT, Thompson SH, Stricker SA, Patton C, Bonaventura J, Epel D. NO is necessary and sufficient for egg activation at fertilization. Nature 2000;406:633–636. [PubMed: 10949304]
37. Thaler CD, Epel D. Nitric oxide in oocyte maturation, ovulation, fertilization, cleavage and implantation: a little dab'll do ya. Curr Pharm Des 2003;9:399–409. [PubMed: 12570817]
38. Alonso JM, Stepanova AN, Leisse TJ, Kim CJ, Chen H, Shinn P, Stevenson DK, Zimmerman J, Barajas P, Cheuk R, et al. Genome-wide insertional mutagenesis of *Arabidopsis thaliana*. Science 2003;301:653–657. [PubMed: 12893945]
39. Clough SJ, Bent AF. Floral dip: a simplified method for *Agrobacterium*-mediated transformation of *Arabidopsis thaliana*. Plant J 1998;16:735–743. [PubMed: 10069079]
40. Copenhaver GP, Keith KC, Preuss D. Tetrad analysis in higher plants. A budding technology. Plant Physiol 2000;124:7–16. [PubMed: 10982416]
41. Johnson-Brousseau SA, McCormick S. A compendium of methods useful for characterizing *Arabidopsis* pollen mutants and gametophytically-expressed genes. Plant J 2004;39:761–775. [PubMed: 15315637]
42. Palmer AE, Giacomello M, Kortemme T, Hires SA, Lev-Ram V, Baker D, Tsien RY. Ca2+ indicators based on computationally redesigned calmodulin-peptide pairs. Chem Biol 2006;13:521–530. [PubMed: 16720273]
43. Szabados L, Charrier B, Kondorosi A, Debruijn FJ, Ratet P. New plant promoter and enhancer testing vectors. Molecular Breeding 1995;1:419–423.
44. Hellens RP, Edwards EA, Leyland NR, Bean S, Mullineaux PM. pGreen: a versatile and flexible binary Ti vector for *Agrobacterium*-mediated plant transformation. Plant Mol Biol 2000;42:819–832. [PubMed: 10890530]

45. Fan LM, Wang YF, Wang H, Wu WH. *In vitro Arabidopsis* pollen germination and characterization of the inward potassium currents in *Arabidopsis* pollen grain protoplasts. J Exp Bot 2001;52:1603–1614. [PubMed: 11479325]

46. Frietsch S, Wang YF, Sladek C, Poulsen LR, Romanowsky SM, Schroeder JI, Harper JF. A cyclic nucleotide-gated channel is essential for polarized tip growth of pollen. Proc Natl Acad Sci USA 2007;104:14531–14536. [PubMed: 17726111]

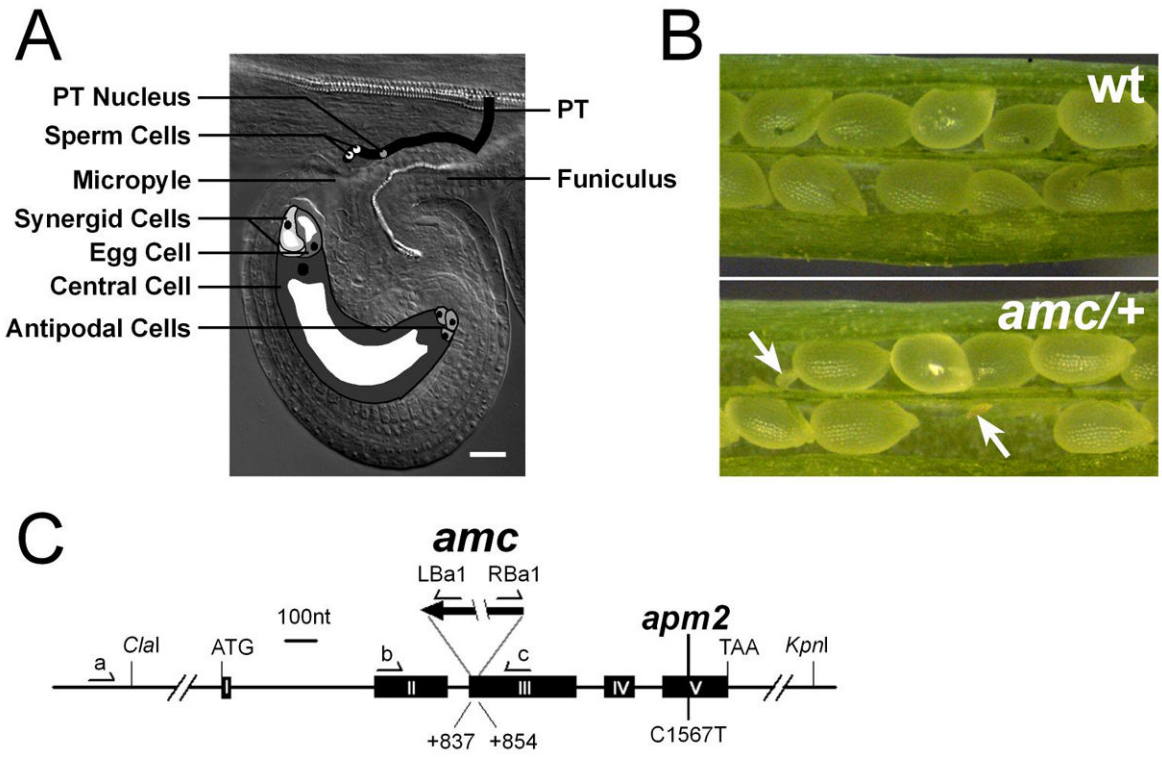

Figure 1. Siliques of *amc*/+ mutant lack homozygous individuals

(A) Schematic drawing of male and female gametophytes during fertilization in *Arabidopsis thaliana.* The pollen tube (PT) enters the ovule through the micropyle, an opening leading to the seven-celled haploid female gametophyte and reaches the receptive synergid cell in which it will discharge its sperm cells, a process called pollen tube reception. During double fertilization, one sperm cell fuses with the egg cell, which will give rise to the zygote, while the second sperm will fertilize the central cell to induce endosperm formation. Scale Bar is 20 μm.

(B) In contrast to wild-type siliques (top), siliques of self-pollinated *amc*/+ plants frequently contained degenerating ovules (bottom, white arrows).

(C) Exon/Intron organization of the *APM2/AMC* locus (At3g07560) and position of the T-DNA in the *amc*/+ mutant. Positions of the primers used to genotype the *amc*/+ mutant and position of the point mutation in the weak *apm2* allele [15] are indicated.

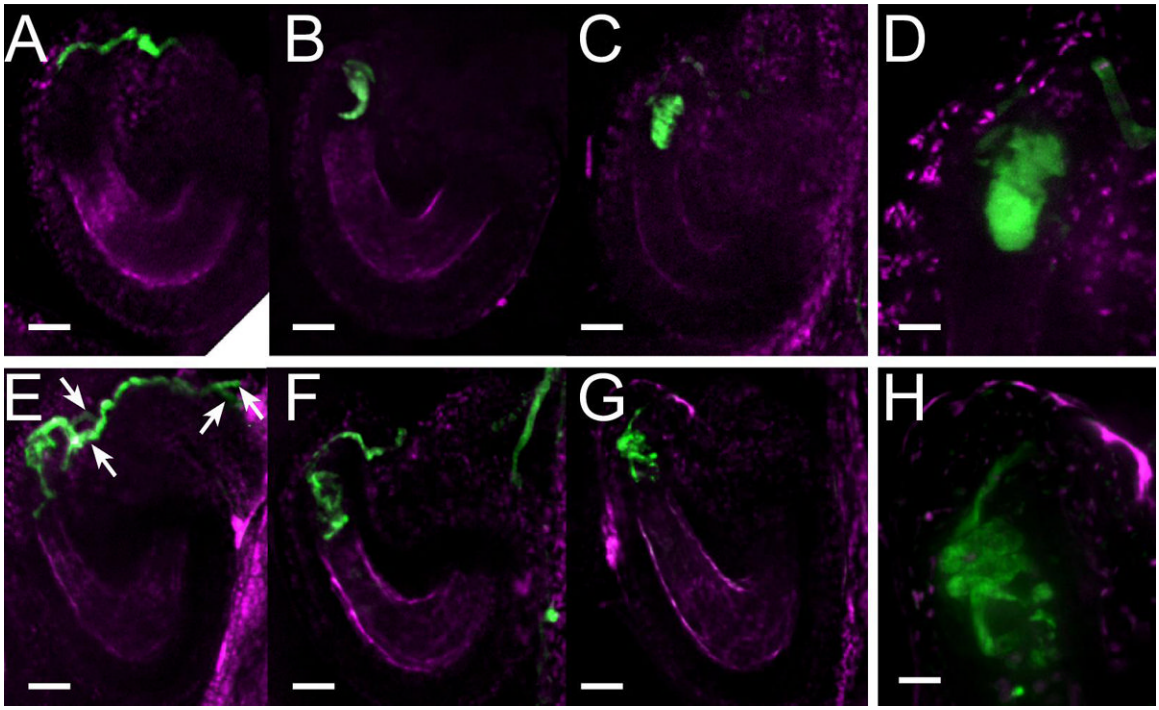

Figure 2. The *amc* mutation disrupts pollen tube growth arrest and discharge

(A–H) Examination by confocal microscopy of YFP-expressing pollen 19–24h after manual pollination during wild-type (A–D) and *amc* mutant (E–H) pollen/ovule interactions. Fluorescence from the YFP expressed in pollen tubes is shown in green while the autofluorescence from the ovule tissues is shown in magenta.

(A) A wild-type pollen tube reaching the micropylar side of the synergid cells.

(B,C) Two examples of wild-type pollen tube discharges. At the extremity of the PT, the fluorescence assumes the shape of the receptive synergid cell in which the pollen tube has released its content.

(D) Close-up of (C).

(E–G) Three examples of continued growth of presumably an *amc* pollen tube reaching an *amc* ovule (see Results and Discussion). The mutant pollen tube while reaching the micropylar part of the synergid cells does not discharge. It keeps growing by coiling and branching (F,G) and the pollen tube tips can be spotted past the synergid cells of the mutant ovule (E,F). Among these mutant interactions, two pollen tubes can be frequently observed within a presumed *amc* ovule (E, white arrows).

(H) Close-up image of the coiled pollen tube shown in (G). Note how the pollen tube coils and branches making the fluorescence outlines rougher than in (D).

Scales bars are 23 μm for A–C, E–G and 7 μm for D,H.

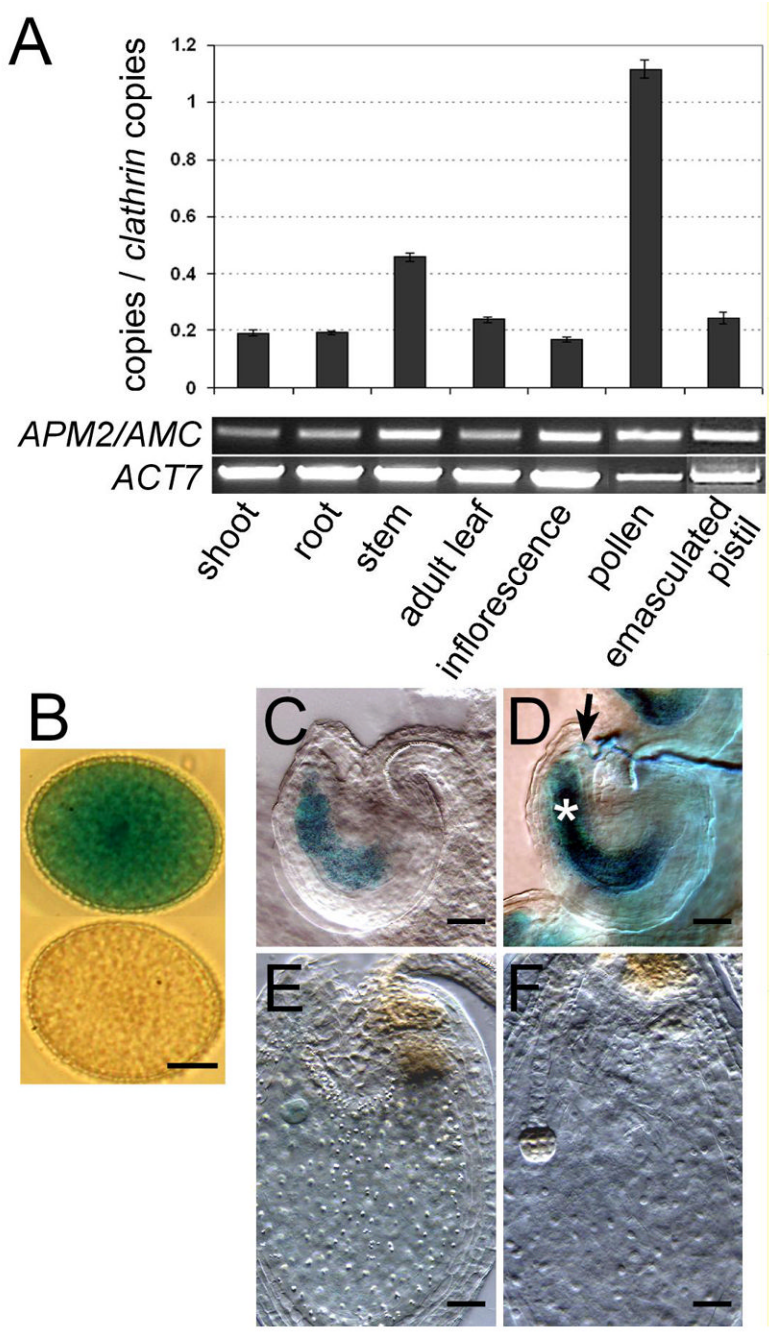

Figure 3. *APM2/AMC* expression pattern supports its role during fertilization

(A) Semi-quantitative RT-PCR (bottom, 31 cycles) and quantitative real-time (RT)-PCR (top) analyses of *APM2/AMC* expression in different organs/tissues. *ACTIN7* (At5g09810) was used as a control for RT-PCR analysis. For quantitative real-time (RT)-PCR experiments, *Clathrin* (At4g24550) was used as an internal control and each data point indicates the average of three independent experiments ± SEM. In line with the microarray data (Figure S4A), these analyses indicated that *APM2/AMC* is preferentially expressed in mature pollen grains. (B–F) Histochemical localization of *GUS* reporter gene expression driven by the *APM2/AMC* promoter in pollen grains (B) and during fertilization (C–F). (B) one hour GUS-stained *pAMC-GUS* pollen (top) and untransformed wild-type pollen (bottom) grains. Scale bar is 5

μm. (C–F) *GUS* expression in a mature female gametophyte before (C), during (D), 24h after (E) and 48h (F) after fertilization (12h GUS staining). During fertilization (D), both male (arrow) and female (asterisk) gametophytes are strongly stained. Note how strongly the GUS activity dropped after fertilization (E, F). Scale bars are 28 μm for C–F. See also Supplemental Data and Figure S4F.

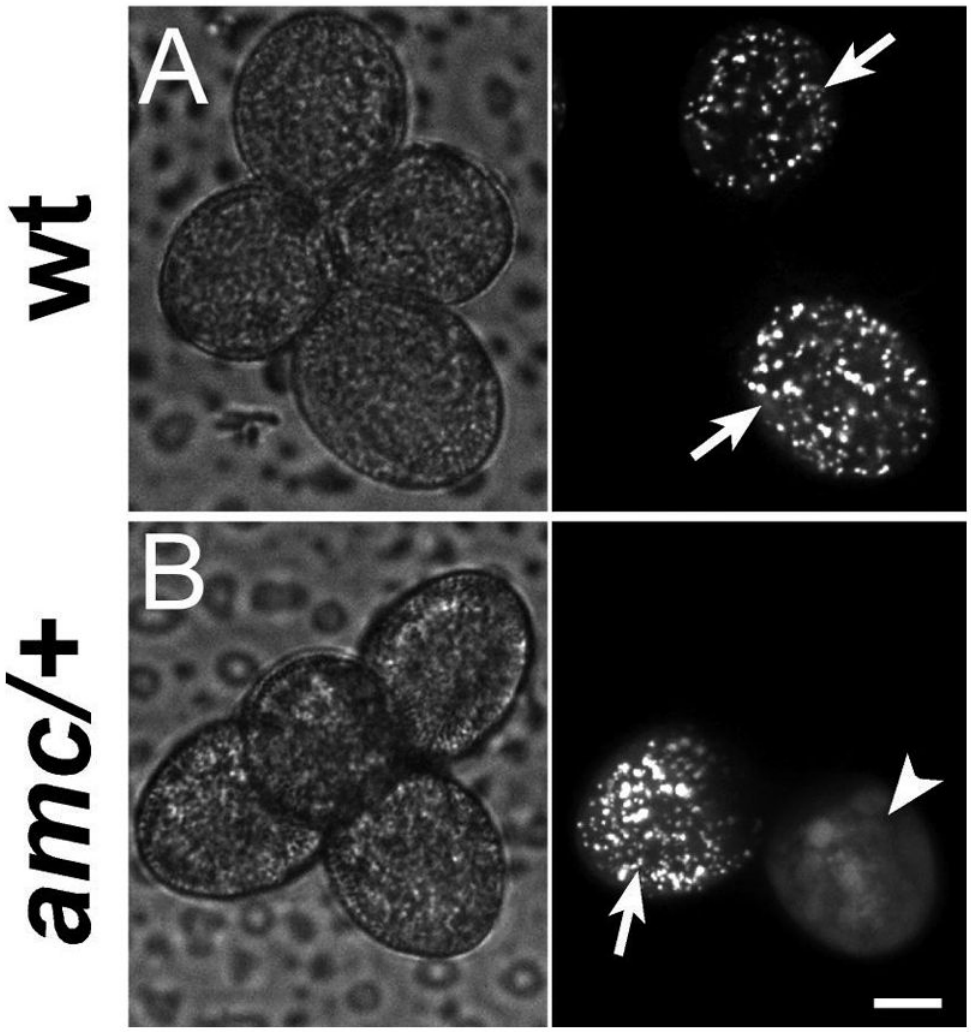

Figure 4. PTS1-dependent protein import into peroxisomes is completely impaired in *amc* mutant pollen

Examination by confocal microscopy of pollen tetrads of wild-type (A) and *amc*/+ (B) plants heterozygous for the peroxisomal pLAT52-CFP-PTS1 marker. Left panels, bright light; right panels, CFP filter. Scale bar is 10 μm.

(A) In wild-type tetrads, all the fluorescent pollen grains (half of the total grains) exhibited a fluorescence with a peroxisome-like punctuated pattern (white arrows) indicative of a normal PTS1-dependent import into peroxisomes.

(B) In *amc*/+ tetrads, in a 1:1 expected ratio for segregation of the fully penetrant *amc* mutation, fluorescent pollen grains exhibited fluorescence either in a punctuated pattern as in wild-type (arrow) or exclusively in the cytosol (arrowhead). In this latter case, note how peroxisomes can no longer be discerned, indicating complete impairment of PTS1-dependent import into peroxisomes (see also Figure S7 for pollen tubes growing *in vitro*).

Table 1

Segregation analysis of the *amc* mutation by PCR-based genotyping

female × male	**+/+**	***amc*/+**	***amc*/*amc***	**% *amc*/+**	**%TE**	**% of non-aborted ovules in F1 siliques**
amc/+ × *amc*/+	218	306	0	**58.4**	**nd**	**76** (n=891)
amc/+ × +/+	29	24	0	**45.3**	**82.8**	**94** (n=605)
+/+ × *amc*/+	65	33	0	**33.7**	**50.8**	**93** (n=923)
+/+ × +/+	nd	nd	nd	nd	nd	**94** (n=712)